

## Fabrication of Hybrid NiO/ACF/TiO<sub>2</sub> Composites and Their Photocatalytic Activity Under Visible Light

Ze-Da Meng, Sang-Bum Han, Doo-Hwan Kim, Chong-Yeon Park, and Won-Chun Oh<sup>†</sup>

Department of Advanced Materials & Science Engineering, Hanseo University, Seosan 356-706, Korea

(Received March 25, 2011; Revised April 9, 2011; Accepted April 21, 2011)

### ABSTRACT

Nickel oxide-doped ACF and TiO<sub>2</sub> composites (NiO/ACF/TiO<sub>2</sub>) were prepared by a sol-gel method. The composite obtained was characterized by BET surface area measurements, X-ray diffraction, transmission electron microscopy and energy dispersive X-ray analysis. A methylene blue (MB) solution under visible light irradiation was used to determine their photocatalytic activity. Excellent photocatalytic degradation of the MB solution was observed using the TiO<sub>2</sub>, Ti-ACF and NiO/ACF/TiO<sub>2</sub> composite under visible light.

**Key words :** ACF, Nickel oxide, Visible light, TiO<sub>2</sub>, Photocatalytic

### 1. Introduction

In recent years, the photocatalytic degradation of various kinds of organic and inorganic pollutants using semiconductor powders as photocatalysts has been extensively studied.<sup>1-4)</sup> Owing to its relatively high photocatalytic activity, biological and chemical stability, low cost, non-toxic nature and long-term stability, TiO<sub>2</sub> has been widely used as a photocatalyst.<sup>5)</sup> However, the photocatalytic activity of TiO<sub>2</sub> (the band gap of anatase TiO<sub>2</sub> is 3.2 eV and it can be excited by photons with wavelengths below 387 nm) is limited to irradiation wavelengths in the UV region; thereby the effective utilization of solar energy is limited to about 3-5% of the total solar spectrum.<sup>6-8)</sup> Some problems still remain to be solved. One approach is to dope transition metals into TiO<sub>2</sub>, and another is to form coupled photocatalysts.<sup>9-11)</sup> Recently, it was found that substitution of a non-metallic element, such as nitrogen, fluorine, sulfur, carbon, etc., for oxygen in the TiO<sub>2</sub> lattice is more efficient in improving its photocatalytic activity in the visible region.<sup>12,13)</sup>

Activated carbon fiber (ACF), widely used as an effective adsorbent in treating polluted water and gas, was introduced as a support for a TiO<sub>2</sub> photocatalyst in some studies. ACF is one kind of highly microporous carbon materials, having a higher surface area, larger pore volume and a more uniform micropore size distribution than granular activated carbon. However, so far there have been only a few reports that studied preparation methods and applications for ACF TiO<sub>2</sub> composites. In another aspect of improving photocatalytic activity, reducing the recombination of holes and electrons by doping TiO<sub>2</sub> with transition metals

has been proposed as the most common method.<sup>14-16)</sup>

It is known that NiO is a p-type semiconductor, and TiO<sub>2</sub> is an n-type semiconductor. The band gap of NiO is 3.6-4.0 eV.<sup>17)</sup> When p-type NiO and n-type TiO<sub>2</sub> integrates, a p-n junction will be formed between the p-NiO and n-TiO<sub>2</sub>. Theoretically, the photogenerated electrons and holes are separated efficiently, and the photocatalytic activity is enhanced.<sup>18,19)</sup>

In this study, the p-n junction photocatalyst NiO/ACF/TiO<sub>2</sub> was prepared by a sol-gel method using different amounts of Ni(OH)<sub>2</sub> and TOS as the raw material, and the photocatalyst was characterized by X-ray diffraction (XRD), scanning electron microscopy (SEM) and energy dispersive X-ray (EDX). The photocatalytic efficiencies of these composites were evaluated according to the photo-degradation of the MB solutions.

### 2. Experimental

#### 2.1. Materials

Self-made ACF used as a precursor fiber material was prepared from commercial PAN-based carbon fibers (T-300 Amoco, USA). The carbon fibers were activated by steam diluted with nitrogen in a cylinder quartz glass tube at a temperature of 1073 K for 30 min. TiOSO<sub>4</sub>·xHO<sub>2</sub> (TOS) were purchased from Solvachim and Merck, respectively. H<sub>2</sub>O<sub>2</sub> was purchased from Daejung Chemicals Metals Co., Ltd. and was used to dissolve the TOS. Methylene blue was supplied by Duksan Pure Chemical Co., Ltd. Nickelous hydroxide [Ni(OH)<sub>2</sub>] was supplied from Duksan Pure Chemical Co. (Korea).

#### 2.2. Preparation of NiO/ACF/TiO<sub>2</sub> composites

These ACFs were washed with deionized water and dried for 24 h at an ambient temperature. The ACFs were pulverized by a pulverizer. 8 g of carbon fiber materials were ball

<sup>†</sup>Corresponding author : Won-Chun Oh  
E-mail : wc\_oh@hanseo.ac.kr  
Tel : +82-41-660-1337 Fax : +82-41-688-3352

**Table 1.** Nomenclature of the Samples Prepared with the Photocatalysts

Preparation method	Nomenclatures
ACF + TOS	Ti-ACF
ACF + 0.025 M Ni(OH) <sub>2</sub> + TOS	NiACFT1
ACF + 0.05 M Ni(OH) <sub>2</sub> + TOS	NiACFT2

milled for 48 h at room temperature in a laboratory tumbling ball mill, and then the mechano-chemically carbon materials were obtained using a laboratory Pulverisette 6 mono-planetary high energy mill (Idar-Oberstein, Frisch, Germany) for 1 h with ZrO<sub>2</sub> ball (1 mm × 300 g). H<sub>2</sub>SO<sub>4</sub> and H<sub>3</sub>PO<sub>4</sub> mixed solution (with a volume ratio of 70:30, solution A) was used to oxidize the ACF particles. 3 g of pulverized ACF was mixed with 100 ml of solution A, stirring 7-8 h and flushed with distilled water 3 times and dried at 323 K. Oxidized ACF was formed.

For treating the Ni sources in the ACF matrix, 0.025 M and 0.05 M Ni(OH)<sub>2</sub> solutions were mixed with oxidized ACF. This mixture was heated under reflux in air and stirred at 343 K for 5 h using a magnetic stirrer in a vial. The NiO/ACF compounds were obtained after heat treatment at 773 K for 1 h.

The Ni treated ACF composites were placed in a mixing solution of TOS and oxydol (H<sub>2</sub>O<sub>2</sub>) solution. The solutions were then homogenized under reflux at 343 K for 5 h, while being stirred in a vial. After stirring, the solution was transformed into NiO/ACF/TiO<sub>2</sub> gels, which were heat treated at 873 K to produce the NiO/ACF/TiO<sub>2</sub> composites (NiACFT1 and NiACFT2). Ti-ACF was prepared with the same method as above, using oxidized ACF and TOS oxydol solution (showed in Table 1).

### 2.3. Characterization of NiO/ACF/TiO<sub>2</sub> compounds

XRD (Shimatz XD-D1, Japan) was used for crystal phase identification and to estimate the anatase ratio of TiO<sub>2</sub> and estimate the crystal phase of NiO. The XRD patterns were obtained at room temperature using Cu K $\alpha$  radiation. SEM (JOEL, JSM-5200, Japan) was used to observe the surface state and porous structure of the NiO/ACF/TiO<sub>2</sub> composites. The elemental composition of the NiO/ACF/TiO<sub>2</sub> composites was examined by EDX. SEM was used to observe the surface state and structure of the CdS-C<sub>60</sub>/TiO<sub>2</sub> composites using a scanning electron microscope (JSM-5200 JOEL, Japan). The Brunauer-Emmett-Teller (BET) surface area was determined by N<sub>2</sub> adsorption measurements at 77 K (Monosorb, USA).

### 2.4. Photocatalytic tests

A specified quantity of the NiO/ACF/TiO<sub>2</sub> composites was added to 50 ml of MB solution. The reactor was placed in the dark for 2 h to allow the maximum adsorption of MB molecules to the NiO/ACF/TiO<sub>2</sub> composite particles. In all the experiments, the initial concentration of the MB was  $1 \times 10^{-5}$  mol/L, and the amount of the NiO/ACF/TiO<sub>2</sub> compos-

ite was 0.05 g/(50 ml solution). After adsorption, photodecomposition of the MB solution was performed under visible light in a dark-box to ensure that the reactor was irradiated by a single light source. The visible light source used was an 18 W lamp with the main emission wavelength at 360 nm. Visible light irradiation of the photoreactor was performed for 10 min, 30 min, 60 min, 90 min, 120 min, and 150 min. The experiments were performed at room temperature. In the process of MB degradation, a glass reactor (bottom area = 20 cm<sup>2</sup>) was used and the reactor was placed on a magnetic churn dasher. Samples were then withdrawn regularly from the reactor and the dispersed powders were removed by a centrifuge. The MB concentration in the solution was then determined as a function of the irradiation time from the change in absorbance at a wavelength of 660 nm. After treatment with the centrifuge, the centrifugalizations were analyzed using a UV-vis spectrophotometer.

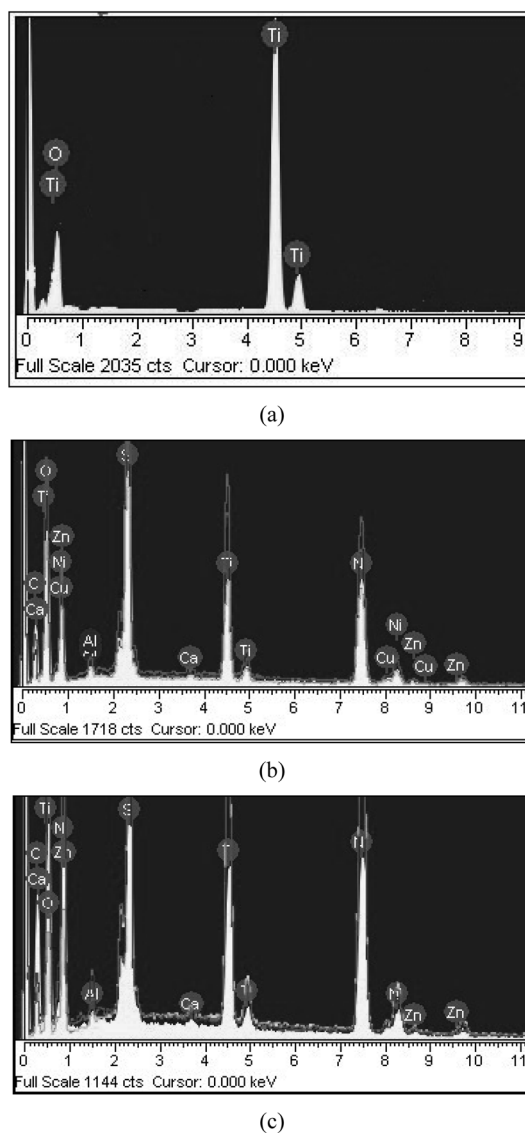
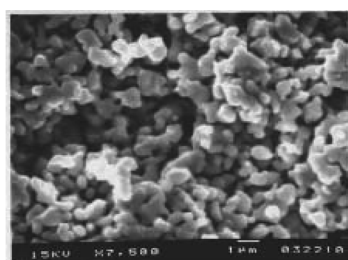


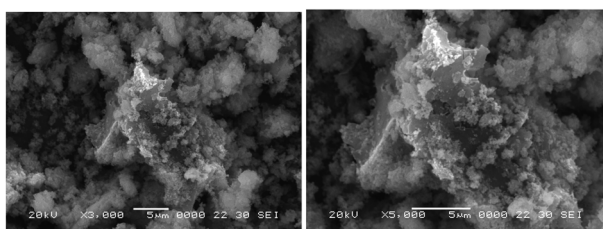
**Fig. 1.** EDX elemental microanalysis of TiO<sub>2</sub>: (a) NiACFT1, (b) NiACFT2, and (c) composites.

**Table 2.** EDX Elemental Microanalysis and BET Surface Area

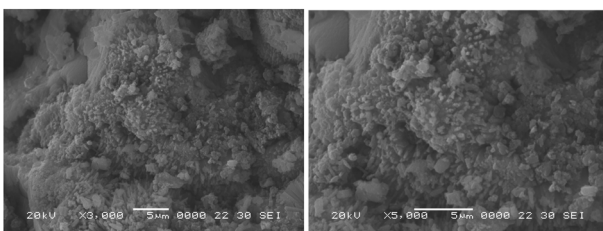
Samples	TiO <sub>2</sub>	ACF	Ti-ACF	NiACFT1	NiACFT2
BET	17.1	327.3	273.5	186.0	134.6
Samples	C	O	Ni	Ti	Impurity
NiACFT1	27.05	34.21	22.50	14.31	1.93
NiACFT2	28.16	31.04	25.10	13.00	2.70



(a)



(b)



(c)

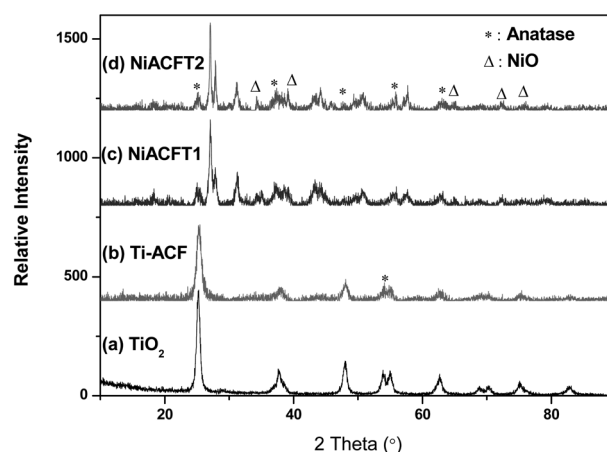
**Fig. 2.** SEM images of TiO<sub>2</sub>: (a) NiACFT1, (b) NiACFT2, and (c) composites.

### 3. Results and Discussion

#### 3.1. Structure and morphology of composites

Fig. 1 shows the results of EDX examinations of the surface of the NiACFT1 and NiACFT2 compounds. The elemental composition of these samples was analyzed and the characteristic elements were identified. Fig. 1 shows strong K $\alpha$  and K $\beta$  peaks from Ti at 4.51 and 4.92 keV, whereas a moderate K $\alpha$  peak for O appears at 0.52 keV.<sup>20</sup> In addition to the above peaks, Ni was also observed. Fig. 1 presents the quantitative microanalysis of C, O, Ti and Ni as the major elements for the composites by EDX. Table 1 lists the composition ratios of the samples. There were some small impurities, which are believed to have been introduced from the unpurified yttrium nitrate.<sup>21</sup> In the case of most samples, carbon and titanium were present as major elements with small quantities of oxygen in the composite (shown in Table 2).

Fig. 2 shows the SEM images of the micro-surface struc-

**Fig. 3.** The XRD patterns of TiO<sub>2</sub>, Ti-ACF, NiACFT1, and NiACFT2 composites.

tures and the morphology of the NiACFT1 and NiACFT2 compounds. The TiO<sub>2</sub> and nickel oxide particles were coated uniformly over the ACF surface, which led to an increase in nanoparticle size. Zhang et al. reported that a good dispersion of small particles could provide more reactive sites for the reactants than aggregated particles.<sup>22,23</sup> The surface roughness appears to be high due to some grain aggregation. Figs. 2 (a), (b) and (c) show the SEM images of pure TiO<sub>2</sub>, NiACFT1 and NiACFT2, respectively. The level of aggregation increased with an increasing content of nickel oxide. Comparing Figs. (a), (b) and (c), we can find that when NiO was added, the aggregation became strong. Ni can enhance aggregation.<sup>24</sup>

Table 1 lists the BET surface areas of the samples. The BET surface areas of pristine ACF, TiO<sub>2</sub>, and Ti-ACF, as well as the prepared NiACFT1 and NiACFT2 were 327.3 m<sup>2</sup>/g, 17.1 m<sup>2</sup>/g, 273.5 m<sup>2</sup>/g, 186.0 m<sup>2</sup>/g and 134.6 m<sup>2</sup>/g, respectively. The TiO<sub>2</sub> and nickel oxide particles were introduced to the pore of the ACF, which decreased the BET surface area. The Ti-ACF sample had the largest area, which can affect the adsorption reaction. The BET surface area of the photocatalyst Ti-ACF decreased by 31.99% when Ti-ACF particles were doped by nickel oxide. This is because nickel oxide particles fill the pores of the Ti-ACF particles, thereby reducing the pore size and pore volume of Ti-ACF particles (showed in Table 2).<sup>25-28</sup>

Fig. 3 shows XRD patterns of the TiO<sub>2</sub>, Ti-ACF and NiO/ACF/TiO<sub>2</sub> composites. After heat treatment at 873 K, major peaks were observed at 25.3, 37.9, 48.0, 53.8, 54.9, and 62.5° 2 $\theta$ , which were assigned to the (101), (004), (200), (105), (211), and (204) planes of anatase, indicating that the prepared TiO<sub>2</sub> is anatase.<sup>29</sup> These results suggest that NiO/ACF/TiO<sub>2</sub> also has a pure anatase phase structure with the current preparation conditions. In the Ti-ACF and NiO/ACF/TiO<sub>2</sub> composite's XRD pattern the intensity of the peaks about TiO<sub>2</sub> was decreased. The XRD pattern shows the characteristic peaks of NiO (bunsenite). Additional NiO diffraction peaks for the (111), (200), (220), (311) and (222)

planes were observed at  $36.9^\circ$ ,  $42.9^\circ$ ,  $62.5^\circ$ ,  $75.0^\circ$  and  $79.0^\circ$  ( $2\theta$ ), respectively.<sup>30-32</sup> The peaks of NiO were also observed in the XRD pattern of NiO/ACF/TiO<sub>2</sub> compounds. Compared to the XRD patterns of NiACFT1 and NiACFT2, when the content of Ni increased, the intensity of the characteristic peaks about NiO increased and the intensity of the characteristic peaks about TiO<sub>2</sub> decreased. There are few other peaks which are believed to have been introduced from the unpurified nickelous hydroxide and TiOSO<sub>4</sub>·xH<sub>2</sub>O.

### 3.2. Photocatalytic activity

Fig. 4 shows the relative concentration of the degraded MB solution by the different samples after irradiation under visible light by different times. There are two steps during degradation of the MB solution. The first step is adsorption, followed by exposure to visible light to degrade the MB solution. Pure TiO<sub>2</sub> had no photocatalytic effect under visible light and because of its poor BET surface area, there was little MB adsorption.<sup>33</sup> Ti-ACF compounds have the highest BET surface area, which can enhance the

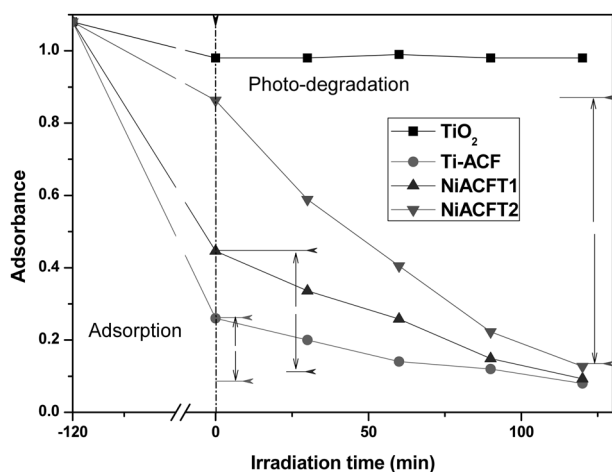


Fig. 4. Absorbance and photo-degradation of the MB solution by different samples under visible light irradiation.

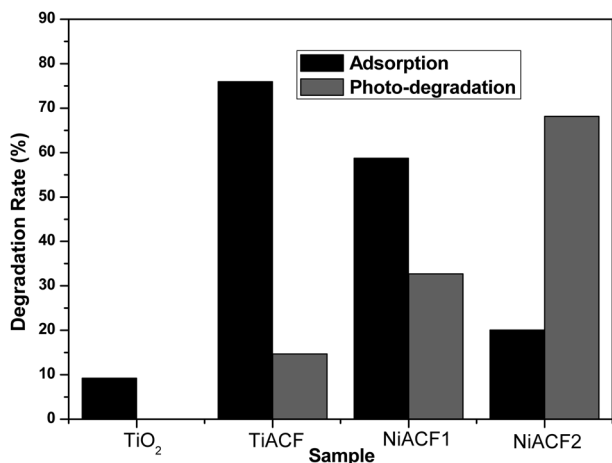


Fig. 5. Adsorption and photo-degradation effect.

adsorption of MB. Therefore, Ti-ACF compounds have the best adsorption effect in the first step. Fig. 5 shows the adsorption and photo-degradation effect. From Fig. 5 we can see Ti-ACF adsorbed 75.92% MB molecules, and TiO<sub>2</sub> compounds adsorbed 9.23% MB molecules due to the relative minimum BET surface area. NiACFT1 had a better adsorption effect than NiACFT2.

At the photo-degradation step, due to the incompetence of TiO<sub>2</sub> in the visible region, TiO<sub>2</sub> particles had no photo-degradation effect under visible light irradiation. From Fig. 5 and Table 3, Ti-ACF, NiACFT1 and NiACFT2 degraded 14.67%, 32.69% and 68.15% MB molecules, respectively. The photo-degradation rate was increased by 18.02% when Ni was added, and the photo-degradation rate of NiACFT2 increased with an increased content of NiO.

Doping TiO<sub>2</sub> with carbon (ACF) extends the absorption wavelengths from UV to the visible region, which has been ascribed to the introduction of localized electronic states in the bandgap. Carbon acted as a photosensitizer, which could be excited to inject electrons into the conduction band of TiO<sub>2</sub>. Subsequently, the electrons could be transferred to surface-adsorbed oxygen molecules and form superoxide anions, which could further transform to OH and initiate the degradation of MB. This is additional evidence that the removal effect of organic materials in solution was also governed by physisorption by porous ACF.<sup>34-36</sup>

Fig. 4 shows that NiO/ACF/TiO<sub>2</sub> has good photocatalytic activity under visible light. This can be attributed to both the effects of photocatalysis of the supported TiO<sub>2</sub>, the charge transfer and photosensitizing of the ACF; and the introduction of nickel to enhance the photogenerated electrons transfer.

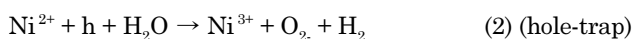
Reactivity of TiO<sub>2</sub> depends on many factors: the adsorption of dye on the catalyst surface, band gap energy, surface area, crystal size, crystallinity and electron-hole recombination rate, so an explanation of the reactivity order is complicated.<sup>35</sup> The addition of nickel oxide on the Ti-ACF photocatalyst surface can enhance the photocatalytic degradation activity, due to the higher efficiency for the electron hole regeneration, and the charge trapping.

The absorption in the visible region is caused by the deviation of NiO from the ideal composition; the nonstoichiometric ratio leads the light absorption centers present, which is a characteristic of a p-type semiconductor.

When p-type NiO and n-type TiO<sub>2</sub> integrates, a p-n junction formed between p-NiO and n-TiO<sub>2</sub>. Theoretically, when a p-type semiconductor NiO and an n-type semiconductor TiO<sub>2</sub> form p-n junctions, an inner electric field will formed at the interface. At equilibrium, the inner electric field makes a p-type semiconductor NiO region have a negative charge, while a TiO<sub>2</sub> region will have a positive charge. Electron-hole pairs may be created on the n-type semiconductor TiO<sub>2</sub> surface, and the photogenerated electron-hole pairs are separated by the inner electric field. The holes flow into the negative field and the electrons move to the positive field. As a result, the photogenerated electrons and holes

are separated efficiently, and the photocatalytic activity is enhanced.<sup>37-39)</sup>

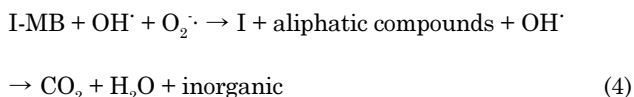
Nickel oxide was used to inhibit electron-hole pair recombination. For this supported catalyst system, charge pair separation was suggested to proceed via electron donation from the TiO<sub>2</sub> frame and the electron-accepting role possessed by nickel ions (electron-trap).



NiO is a *p*-type semiconductor that with excess oxygen in NiO produces a Ni<sup>2+</sup> vacancy, which leads to the creation of a hole on two adjacent Ni<sup>2+</sup> ions, thus producing Ni<sup>3+</sup> ions



Oxidative degradation of azo dyes generally occurs by the attack of hydroxyl radicals, which are known as highly reactive electrophilic oxidants.<sup>40,41)</sup>



(I: adsorption site)

Ti-ACF has a photo-degradation rate under visible light irradiated and NiO/ACF/TiO<sub>2</sub> has a good photo-degradation rate due to the higher efficiency of the electron hole regeneration, and the charge trapping and the inhibition of the electron-hole pair recombination in this system.

## 4. Conclusions

This paper described the preparation and characterization of TiO<sub>2</sub>, Ti-ACF and NiO/ACF/TiO<sub>2</sub> composites. The BET surface area of the Ti-ACF composite was higher than that of NiO/ACF/TiO<sub>2</sub>. XRD revealed the NiO structure and anatase. The NiO/ACF/TiO<sub>2</sub> composite showed the best photocatalytic degradation activity of the MB solution under visible light irradiation. This was attributed to the three different effects: the photocatalytic reaction of the supported TiO<sub>2</sub>, inhibition of electron-hole pair recombination by the Ni particles and the energy transfer effects of ACF, such as electrons and light. When the content of nickel oxide increased, the photo-degradation rate increased.

## REFERENCES

1. F. J. Zhang, M. L. Chen, K. Zhang, and W. C. Oh, "Visible Light Photoelectrocatalytic Properties of Novel Yttrium Treated Carbon Nanotube/titania Composite Electrodes," *Bull. Kor. Chem. Soc.*, **31** 133-39 (2010).
2. M. L. Chen, F. J. Zhang, K. Zhang, Z. D. Meng, and W. C. Oh, "Preparation of Carbon-TiO<sub>2</sub> Composites by Using Different Carbon Sources with Titanium n-butoxide and Their Photocatalytic Activity," *Elas. Comp.*, **45** 25-31 (2010).
3. Z. D. Meng, K. Zhang, and W. C. Oh, "Preparation of Fe-

- AC/TiO<sub>2</sub> Composites and pH Dependence of Their Photocatalytic Activity for Methylene Blue," *J. Kor. Cry. Grow. Cry. Tech.*, **19** 268-76 (2009).
4. Y. Yang, X. Li, J. Chen, and L. Wang, "Titanium Dioxide Mediated Photocatalyzed Degradation of a Textile Dye Derivative, Acid Orange 8, in Aqueous Suspensions," *J. Photochem. Photobiol. A: Chem.*, **163** 517-22 (2004).
5. J. M. Herrmann and C. Guillard, "Photocatalytic Degradation of Pesticides in Agricultural Used Waters," *C. R. Acad. Sci. Paris, Ser. IIC*, **3** 417-22 (2000).
6. M. R. Hoffmann, S. T. Martin, W. Choi, and D. W. Bahnemann, "Environmental Applications of Semiconductor Photocatalysis," *Chem. Rev.*, **95** 69-6 (1995).
7. D. Duonghong, E. Borgarello, and M. Gratzel, "Dynamics of Light-induced Water Cleavage in Colloidal Systems," *J. Am. Chem. Soc.*, **103** 4685-90 (1981).
8. W. C. Oh, A. R. Jung, and W. B. Ko, "Characterization and Relative Photonic Efficiencies of a New Nanocarbon/TiO<sub>2</sub> Composite Photocatalyst Designed for Organic Dye Decomposition and Bactericidal Activity," *Mater. Sci. Eng., C* **29** 1338-47 (2009).
9. W. C. Oh, J. H. Son, F. J. Zhang, and M. L. Chen, "Fabrication of Ni-AC/TiO<sub>2</sub> Composites and their Photocatalytic Activity for Degradation of Methylene Blue," *J. Kor. Ceram. Soc.*, **46** [1] 1-9 (2009).
10. F. J. Zhang and W. C. Oh, "Photoelectrocatalytic Properties of Mo-CNT/TiO<sub>2</sub> Composite Electrodes Under Visible Light," *Asian J. Chem.*, **23** 372-76 (2011).
11. H. S. Li, Y. P. Zhang, S. Y. Wang, Q. Wu, and C. H. Liu, "Study on Nanomagnets Supported TiO<sub>2</sub> Photocatalysts Prepared by a sol-gel Process in Reverse Microemulsion Combining with Solvent-thermal Technique," *J. Hazard. Mater.*, **169** 1045-53.
12. F. J. Zhang, J. Liu, M. L. Chen, and W. C. Oh, "Photoelectrocatalytic Degradation of Dyes in Aqueous Solution using CNT/TiO<sub>2</sub> Electrode," *J. Kor. Ceram. Soc.*, **46** [3] 263-70 (2009).
13. S. Livraghi, M.C. Paganini, E. Giamello, A. Selloni, C.D. Valentin, and G. Pacchioni, "Origin of Photoactivity of Nitrogen-doped Titanium Dioxide Under Visible Light," *J. Am. Chem. Soc.*, **128** 15666-71 (2006).
14. Y. Park, W. Y. Kim, H. W. Park, T. Tachikawa, T. Majima, and W. Y. Choi, "Carbon-doped TiO<sub>2</sub> Photocatalyst Synthesized without Using an External Carbon Precursor and the Visible Light Activity," *Appl. Catalysis B: Envi.*, **91** 355-62 (2009).
15. W. C. Oh, F. J. Zhang, M. L. Chen, Y. M. Lee, and W. B. Ko, "Characterization and Relative Photonic Efficiencies of a New Fe-ACF/TiO<sub>2</sub> Composite Photocatalysts Designed for Organic Dye Decomposition," *J. Ind. Eng. Chem.*, **15** 190-95 (2009).
16. W. Zhang, L. D. Zou, and L. Z. Wang, "A Novel Charge-driven Self-assembly Method to Prepare Visible-light Sensitive TiO<sub>2</sub>/activated Carbon Composites for Dissolved Organic Compound Removal," *Chem. Eng. J.*, **168** 485-92 (2011).
17. N. M. Hosny, "Synthesis, Characterization and Optical Band Gap of NiO Nanoparticles Derived from Anthranilic Acid Precursors Via a Thermal Decomposition Route,"

- Polyhedron*, **30** 470-76 (2011).
18. L. L. Ren, Y. P. Zeng, and D. L. Jiang, "The Improved Photocatalytic Properties of P-type NiO Loaded Porous TiO<sub>2</sub> Sheets Prepared Via Freeze Tape-casting," *Sol. Sta. Sci.*, **12** 138-43 (2010).
  19. K. Nabeen, Shrestha, M. Yang, Y. C. Nah, I. Paramasivam, and P. Schmuki, "Self-organized TiO<sub>2</sub> Nanotubes: Visible Light Activation by Ni Oxide Nanoparticle Decoration," *Electrochem. Com.*, **12** 254-57 (2010).
  20. X. W. Zhang, M. H. Zhou, and L. C. Lei, "Preparation of Photocatalytic TiO<sub>2</sub> Coating of Nanosized Particles Supported on Activated Carbon by AP-MOCVD," *Carbon*, **43** 1700-8 (2005).
  21. W. C. Oh, F. J. Zhang, Z. D. Meng, and K. Zhang, "Relative Photonic Properties of Fe/TiO<sub>2</sub>-nanocarbon Catalysts for Degradation of MB Solution Under Visible Light," *Bull. Kor. Chem. Soc.*, **31** 1128-34 (2010).
  22. Y. Yang, X. Li, J. Chen, and L. Wang, "Titanium Dioxide Mediated Photocatalyzed Degradation of a Textile Dye Derivative, Acid Orange 8, in Aqueous Suspensions," *J. Photochem. Photobiol. A: Chem.*, **163** 517-22 (2004).
  23. L. Wu, J.C. Yu, X. Wang, L. Zhang, and J. Yu, "Characterization of Mesoporous Nanocrystalline TiO<sub>2</sub> Photocatalysts Synthesized Via a Sol-solvothermal Process at a Low Temperature," *J. Solid State Chem.*, **178** 321-28 (2005).
  24. S. F. Chen, S. J. Zhang, W. Liu, and W. Zhao, "Preparation and Activity Evaluation of p-n Junction Photocatalyst NiO/TiO<sub>2</sub>," *J. Hazard. Mater.*, **155** 320-26 (2008).
  25. J. Liqiang, S. Xiaojun, X. Baifu, W. Baiqi, C. Weimin, and F. Honggang, "The Preparation and Characterization of La doped TiO<sub>2</sub> Nanoparticles and Their Photocatalytic Activity," *J. Solid State Chem.*, **177** 3375-82 (2004).
  26. M. V. Shankar, K. K. Cheralthan, B. Arabindoo, M. Palanichamy, and V. "Murugesan, Enhanced Photocatalytic Activity for the Destruction of Monocrotophos Pesticide by TiO<sub>2</sub>/H $\beta$ ," *J. Mol. Catal.*, **223** 195-200 (2004).
  27. M. V. Shankar, S. Anandan, N. Venkatachalam, B. Arabindoo, and V. Murugesan, "Fine Route for an Efficient Removal of 2,4-dichlorophenoxyacetic Acid (2,4-D) by Zeolite-supported TiO<sub>2</sub>," *Chemosphere*, **63** 1014-21 (2006).
  28. Z. D. Meng, K. Y. Cho, and W. C. Oh, "Photocatalytic Degradation of Methylene Blue on Fe-fullerene/TiO<sub>2</sub> Under Visible-light Irradiation," *Asian J. Chem.*, **23** 847-51 (2011).
  29. Y. Zhang, H. Zhang, Y. Xu, and Y. Wang, "Europium doped Nanocrystalline Titanium Dioxide: Preparation, Phase Transformation and Photocatalytic Properties," *J. Mater. Chem.*, **13** 2261-65 (2003).
  30. M. Saif and M. S. A. Abdel-Mottaleb, "Titanium Dioxide Nanomaterial Doped with Trivalent Lanthanide Ions of Tb, Eu and Sm: Preparation, Characterization and POTENTIAL APPLICATIONs," *Inorg. Chim. Acta.*, **360** 2863-74 (2007).
  31. A. Neren Okte and O. Yilmaz, "Photodecolorization of Methyl Orange by Yttrium Incorporated TiO<sub>2</sub> Supported ZSM-5," *Appl. Catal. B. Environ.*, **85** 92-102 (2008).
  32. L. Wu, J.C. Yu, X. Wang, L. Zhang, and J. Yu, "Characterization of Mesoporous Nanocrystalline TiO<sub>2</sub> Photocatalysts Synthesized Via a Sol-solvothermal Process at a Low Temperature," *J. Solid State Chem.*, **178** 321-28 (2005).
  33. F. J. Zhang, M. L. Chen, and W. C. Oh, "Electro-chemical Preparation of TiO<sub>2</sub>/CNT Electrolyte and Their Photoelectrocatalytic Effect," *J. Kor. Ceram. Soc.*, **46** [6] 554-60 (2009).
  34. Y. Ao, J. Xu, D. Fu, X. Shen, and C. Yuan, "Low Temperature Preparation of Anatase TiO<sub>2</sub>-Coated Activated carbon," *Colloid Surfaces*, **312** 125-30 (2008).
  35. G. Colon, M. C. Hidalgo, and J. A. Navio, "A Novel Preparation of High Surface Area TiO<sub>2</sub> Nanoparticles from Alkoxide Precursor and Using Activated carbon as Additive," *Catal. Today*, **76** 91-101 (2002).
  36. J. Matos, J. Laine, and J. Herrmann, "Synergy Effect in the Photocatalytic Degradation of Phenol on a Suspended Mixture of Titania and Activated Carbon," *Appl. Catal. B: Environ.*, **18** 281-91 (1998).
  37. S. F. Chen and G. Y. Cao, "The Preparation of Nitrogen-doped Photocatalyst TiO<sub>2</sub>xNx by Ball Milling," *Chem. Phys. Lett.*, **413** 404-9 (2005).
  38. R. Asahi, T. Morikawa, T. Ohwaki, K. Aoki, and Y. Taga, "Visible-light Photocatalysis in Nitrogen-doped Titanium Oxides," *Science*, **293** 269-71 (2001).
  39. Y. S. Chen, J. C. Crittenden, S. Hackney, L. Sutter, and D. W. Hand, "Preparation of a Novel TiO<sub>2</sub>-based p-n Junction Nanotube Photocatalyst," *Environ. Sci. Technol.*, **39** 1201-8 (2005).
  40. Y. Huang, W. K. Ho, Z. H. Ai, X. Song, L. Z. Zhang, and S. C. Lee, "Aerosol-assisted Flow Synthesis of B-doped, Ni-doped and B-Ni-codoped TiO<sub>2</sub> Solid and Hollow Microspheres for Photocatalytic Removal of NO," *Appl. Catal. B: Environ.*, **89** 398-405 (2009).
  41. H. Yu, X. J. Li, S. J. Zheng, and W. Xu, "Photocatalytic Activity of TiO<sub>2</sub> Thin Film Non-uniformly Doped by Ni" *Mater. Chem. Phys.*, **97** 59-63 (2006).